

## Quantum vortex tunneling in $\text{YBa}_2\text{Cu}_3\text{O}_{7-\delta}$ thin films

G. Koren,\* Y. Mor, A. Auerbach, and E. Polturak

*Physics Department, Technion-Israel Institute of Technology, Haifa 32000, Israel*

(Received 5 July 2007; published 31 October 2007)

Cuprate films offer a unique opportunity to observe vortex tunneling effects due to their unusually low superfluid density and short coherence length. Here, we measure the magnetoresistance (MR) due to vortex motion of a long meander line of a superconducting film made of underdoped  $\text{YBa}_2\text{Cu}_3\text{O}_{7-\delta}$ . At low temperatures ( $T$ ), the MR shows a significant deviation from Arrhenius activation. The data are consistent with two dimensional variable range hopping (VRH) of single vortices, i.e.,  $\text{MR} \propto \exp[-(T_0/T)^{1/3}]$ . The VRH temperature scale  $T_0$  depends on the vortex tunneling rates between pinning sites. We discuss its magnitude with respect to estimated parameters of the meander thin film.

DOI: [10.1103/PhysRevB.76.134516](https://doi.org/10.1103/PhysRevB.76.134516)

PACS number(s): 74.25.Fy, 74.25.Qt, 74.72.Bk, 74.78.Bz

Very soon after the discovery of the high temperature superconductors, the resistive transition was observed to broaden under magnetic fields, instead of shifting to lower temperatures.<sup>1</sup> This was explained as due to thermally activated vortex motion at high temperatures just below  $T_c$ , which gave rise to an induced voltage across the superconductor and thereby to a flux flow resistance  $R_{ff}$ . At any given magnetic field in this regime, this resistance has the form of an Arrhenius law,  $R_{ff} \propto \exp[-(U_0/k_B T)]$ , where  $U_0$  is the activation energy which was discussed by several authors.<sup>2-4</sup> Generally, flux flow and flux creep are possible at high temperatures where the pinning is relatively weak compared to the thermal energy. At low temperatures, where the pinning is stronger and thermal activation is much weaker, the dominant mechanism for flux motion is via quantum tunneling. Measurements of magnetic relaxation and transport by Stein *et al.*<sup>5</sup> have shown a signature of quantum flux creep in  $\text{Y}_{1-x}\text{Pr}_x\text{Ba}_2\text{Cu}_3\text{O}_{7-\delta}$  crystals. This behavior, where the creep is temperature independent, was observed in a very limited temperature range of about 2–4 K. Vortex tunneling in a two dimensional (2D) superconductor at temperatures much lower than the transition temperature  $T_c$  was discussed theoretically by Fisher, Tokuyasu, and Young (FTY)<sup>6</sup> and more recently by Auerbach, Arovas, and Gosh (AAG).<sup>7</sup> FTY studied quantum vortex tunneling in 2D films at  $T$  close to zero near the superconductor to insulator glass transition. They found that this tunneling occurs via variable range hopping (VRH), but instead of the usual  $1/3$  power law in the exponent, at high fields they predicted a different behavior where the exponent ranges between  $2/3$  and  $4/5$ . This resulted from taking into account vortex-vortex interactions. At low fields ( $H \ll H_{c2}$ ), AAG calculated the tunneling rate of a single vortex between two pinning sites and the resulting flux tunneling resistivity. They found that this resistivity depends on temperature as the well known VRH in two dimensions, namely,  $\rho \propto \exp[-(T_0/T)^{1/3}]$ . In the present study, we set up an experiment to test this AAG prediction in a thin film of  $\text{YBa}_2\text{Cu}_3\text{O}_{7-\delta}$  (YBCO) patterned into a very long and narrow meander line. We note that in a short microbridge of YBCO of typically a few hundred micrometers length, and under a magnetic field of several tesla, the voltage induced by moving vortices becomes immeasurably small, and in practical terms, a critical current develops already at about

10–20 K below  $T_c$ . This prohibits measurements of  $R_{ff}$  at low bias and low temperatures. In contrast, in a much longer meander line, the total dc component of the voltage generated by moving vortices is large, and a *de facto* resistive state persists down to very low temperatures, thus enabling the vortex tunneling study.

A question still arises as for why quantum vortex tunneling has not been unequivocally identified in low  $T_c$  superconductors. We believe that this is due to the fact that conventional BCS superconductors are generally three dimensional and characterized by a large coherence length and high superfluid density, all of which greatly inhibit vortex tunneling. In contrast, underdoped cuprate films, such as those investigated here, offer a unique system of low superfluid density and quasi-2D superconductivity with very short coherence lengths. According to a recent theoretical work,<sup>7</sup> in such two dimensional “bosonic” superconductors, vortex tunneling can be manifested in terms of deviation from Arrhenius thermal activation of the magnetoresistance. Therefore, observing the  $(T_0/T)^{1/3}$  exponent would be an exciting signature of the bosonic character of cuprate superconductivity as well as a confirmation of short length-scale vortex tunneling effects. Concerning previous experimental results, we note that the phenomenon of vortex quantum creep has been investigated by both magnetization relaxation and transport in three dimensional cuprate crystals.<sup>5</sup> Unfortunately, although a temperature independent relaxation time and voltage drops have been observed at low temperatures, these experiments did not necessarily probe the low current regime where tunneling (rather than above-barrier classical diffusion) is expected to dominate. The transport results explicitly show nonsaturation at low currents, which indicates that no vortex tunneling occurred in the low current, Ohmic regime. In our experiments, we study thin films with low current bias. This ensures that deviation from Arrhenius activation which we find is indeed related to vortex tunneling and not to classical above-barrier motion.

In the present study, we used epitaxial  $c$ -axis oriented films of YBCO, with the magnetic field applied parallel to this axis and perpendicular to the substrate wafer. The films were prepared by 355 nm laser ablation deposition on (100)  $\text{SrTiO}_3$  wafers of  $10 \times 10 \text{ mm}^2$  area. We investigated films of 50 and 100 nm thickness. In order to reduce their contact

resistance, some films were coated with a 20 nm thick gold layer deposited at a high temperature (780 °C) in oxygen ambient. This gold overlayer consists of loosely connected ball-like grains as seen by atomic force microscope images. Its contribution to the resistance versus temperature of the bilayer was nonmetallic and very small. This was verified in a control experiment in which another bilayer of 20 nm gold on 100 nm YBCO was prepared with the YBCO doped to have a very low  $T_c$ . Thus, its resistance could be measured down to very low temperatures. This bilayer was measured as deposited, without patterning. After measuring the resistance, the Au layer was removed using Ar ion milling and the resistance was measured again. A simple calculation of two parallel resistors shows that the resistivity of the gold layer below 10 K was above 5 m $\Omega$  cm. This value is much higher than the resistivity of the 60 K YBCO phase which is about 0.1 m $\Omega$  cm at 100 K. Considering also the 1:5 thickness ratio between the gold and YBCO layers used, we find that the presence of the gold layer changed the resistance of the meander line by about 0.25%, which is negligible. Nevertheless, the aim of obtaining a low contact resistance with the YBCO film where the contact is made normal to the surface was certainly achieved. We note that the magnetoresistance (MR) results measured with and without the gold layer were basically the same. However, those obtained with the gold overcoating were less noisy, and therefore we chose to present them here.

The YBCO films and Au/YBCO bilayers were annealed *in situ* in a controlled oxygen ambient to have a transition temperature of 50–60 K in order to avoid apparent critical currents at low bias where the current should be proportional to the voltage. The films were patterned by deep UV lithography using a poly-methylmethacrylate resist and Ar ion beam milling into a 4 m long meander line. This meander line had 14  $\mu$ m line width with 4  $\mu$ m line spacing on 8  $\times$  9 mm<sup>2</sup> area of the wafer, while the remaining area was used for the four 1.5  $\times$  1.5 mm<sup>2</sup> contacts. In the patterning process, we limited the development time of the photoresist in order to keep it continuous, but this left several shorts, effectively shortening the meander line. In addition, we found that in the patterning process, a few defects were formed in the long meander line which we bridged with small silver paste dots of  $\sim$ 0.5 mm diameter. The gold overcoating layer was also very helpful in improving the contacts to these bridging dots. This bridging procedure and the shorts mentioned before led to a reduced effective length of our meander lines of about 1 m. This length was estimated from the measured resistance, the resistivity, and the cross section area of the bare YBCO meander lines without the gold coating. For the transport measurements, we used the standard four contact technique in a dc mode, and cooling was done in a liquid helium cryostat with a base temperature of 2 K.

The resistance versus temperature results of the meander line are shown in Fig. 1 for zero field cooling (ZFC) and under magnetic fields of 1, 2, 4, and 6 T applied normal to the wafer. One can see the typical behavior characteristic of underdoped YBCO in the 2–300 K temperature range in the inset to this figure. In the main panel, the superconducting

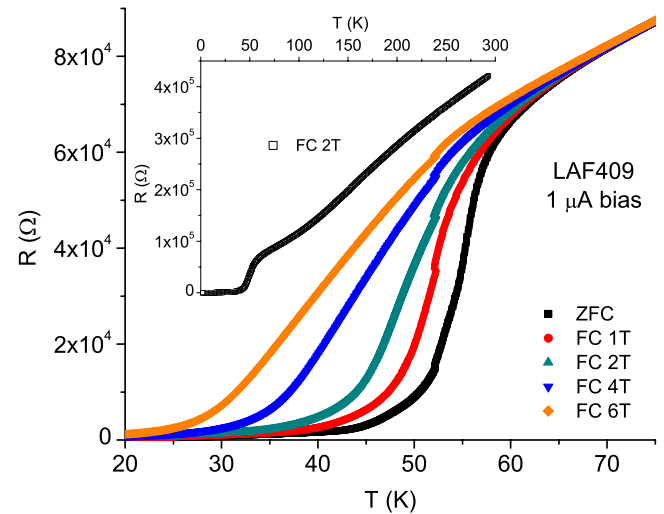


FIG. 1. (Color online) Resistance versus temperature of the YBCO meander line (of  $\sim$ 1 m length and 100 nm  $\times$  14  $\mu$ m cross section area) under various cooling conditions with and without a magnetic field. The resistance of the meander line over a wider temperature range under 2 T field cooling is shown in the inset.

transition temperature range is shown in more detail. The well known thermally activated broadening of the transition under increasing magnetic field is clearly observed, and in addition, a significant resistive tail is seen already at zero field. To see the thermal activation functional dependence and the data at low temperatures, the data of Fig. 1 were replotted in Fig. 2 on a logarithmic scale versus inverse temperature. One can see that the regimes where thermal activation holds are small, about 5 K at 2 T and 7 K at 6 T. The onset of the superconducting transition under ZFC is  $T_c^{onset} = 58$  K, while that of the 6 T field cooled curve is shifted down to about 40 K. This is qualitatively similar to the results of Palstra *et al.*, but with about twice the measured shift

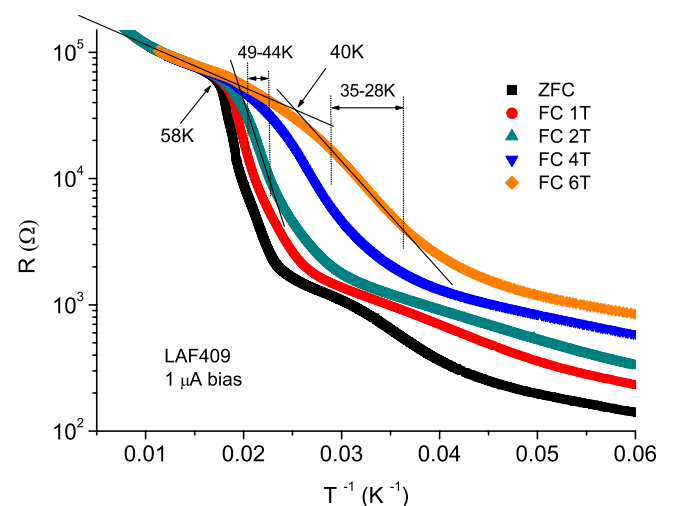


FIG. 2. (Color online) The resistance data of Fig. 1 plotted on a logarithmic scale versus inverse temperature. The standard vortex activation regions where  $R \propto \exp(-U_0/kT)$  are shown for fields of 2 and 6 T.

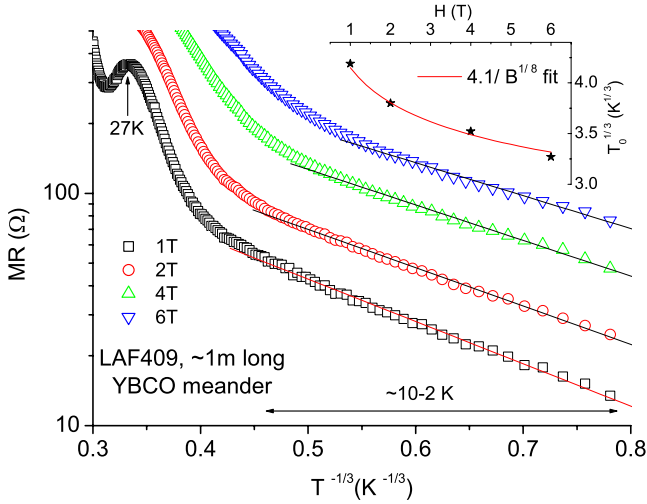


FIG. 3. (Color online) The magnetoresistance  $MR = R(H) - R(0)$  derived from the data of Fig. 1, plotted on a logarithmic scale as a function of  $T^{-1/3}$ . The straight lines are linear fits to the data in the relevant low temperature regimes. In the inset, the slopes of these straight lines (on a logarithmic scale of base  $e$ )  $T_0^{1/3}$  are plotted versus field, together with a fit to  $4.1/B^{1/8}$ .

of the 90 K phase of YBCO single crystals.<sup>8</sup> Also seen in Fig. 2 is a knee in the ZFC curve at 42–34 K just below the main transition. This is a clear signature of weak links, which is very similar to the results on grain boundary junctions.<sup>9</sup> These weak links can be due to defects in the SrTiO<sub>3</sub> substrate which are copied into the epitaxial film, presence of grains of the minority ( $\sim 3\%$ )  $a$ -axis oriented phase, lithography induced defects, and so on. It is therefore clear that any possible vortex tunneling unmasked by other effects could be observed only at temperatures below about 20–30 K.

Next, we study the temperature dependence of the magnetoresistance of the meander line. We use the usual definition of  $MR = R(H) - R(0)$ , where  $R(H)$  and  $R(0)$  are the resistances under a magnetic field  $H$  and at zero field, respectively. Using the magnetoresistance rather than the resistance under field itself has the advantage of eliminating all extrinsic effects such as those contributed by weak links and series resistors of the repairing silver paste dots. We can safely assume that these contributions to the magnetoresistance are small since the relevant defects occupy a very small fraction of the area of the meander line, and their resistance has a much weaker dependence on the perpendicular magnetic field. In Fig. 3, the MR is plotted versus  $T^{-1/3}$  where a linear dependence should indicate VRH in the YBCO planes, while in Fig. 4, the MR is plotted versus  $1/T$  to test for a possible Arrhenius activation process. As one can see, a linear behavior is found in both figures at low temperatures, but the VRH range of Fig. 3 extends over 2–10 K, which is about three times as large as the activation range of 2–5 K as seen in Fig. 4. Although this temperature range is relatively small, the fact that the  $\log(MR) \propto T^{-1/3}$  behavior exists in a significantly larger temperature range suggests that we actually observe VRH as predicted by AAG.<sup>7</sup> Their expression for the magnetoresistivity in a 2D superconductor is

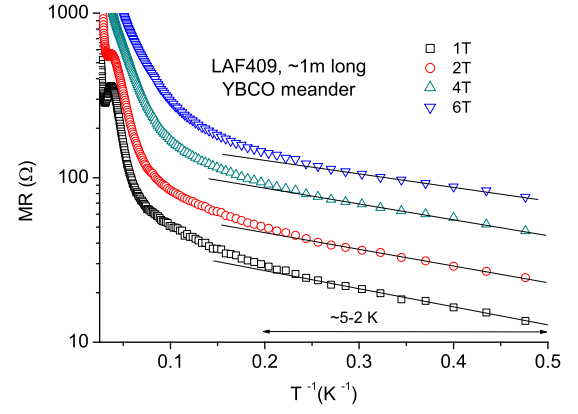


FIG. 4. (Color online) The data of Fig. 3 plotted versus inverse temperature to compare possible standard vortex activation to vortex tunneling by VRH as in Fig. 3. The straight lines are guides for the eye.

$$MR(B, T) = \left(\frac{h}{2e}\right)^2 \gamma_0 [n_v(B)] \exp[-(T_0/T)^{1/3}], \quad (1)$$

where  $\gamma_0$  is the vortex conductivity which depends on the vortex density  $n_v(B)$  and  $T_0$  is given by

$$T_0 = K \delta \bar{V} \left(\frac{\pi n_s}{n_{pin}}\right)^2, \quad (2)$$

where  $K$  is a dimensionless factor of order unity,  $\delta \bar{V}$  is the average variation of the pinning energy,  $n_s$  is the pair density, and  $n_{pin}$  is the pinning site density. It should be noted that this theory strictly applies only to the 2D case, while the actual film has a quasi-three-dimensional (quasi-3D) nature with pancake vortices which have very weak Josephson coupling in the  $c$  direction. The vortices in the film form straight lines which minimize the total pinning potentials of the layers. The minimal instanton action (wave function overlap) for the tunneling events involves motion of an individual vortex which has a pinning site in its close neighborhood. After the tunneling event, the vortex lines up to its new position via classical (above-barrier) relaxation. This satisfies the ingredients of the variable range hopping model, where the mean tunneling distance in a thin film is of the order of  $l_{2D}/\sqrt{N_{layers}}$ , where  $l_{2D}$  is the mean distance between uncorrelated pinning sites in each 2D layer and  $N_{layers}$  is the number of layers in the film. Therefore, for the quasi-3D case of a thin film, Eq. (2) has to be modified by replacing  $n_{pin}$  by  $n_{pin} \times N_{layers}$ , which yields

$$T_0(\text{film}) = K \delta \bar{V} \left(\frac{\pi n_s}{n_{pin} N_{layers}}\right)^2. \quad (3)$$

One can see that for any given field, the results of Fig. 3 at low temperatures are in good agreement with Eq. (1). Although the FTY theory<sup>6</sup> is applicable only at high fields, we also tested their prediction of  $\rho \propto \exp[-(T_0/T)^{2/3}]$ , but this dependence fit our MR data only in the narrow regime of 2–5 K. In the inset of Fig. 3, the  $T_0^{1/3}$  coefficient of Eq. (1) is plotted versus field. We see that this coefficient is not exactly

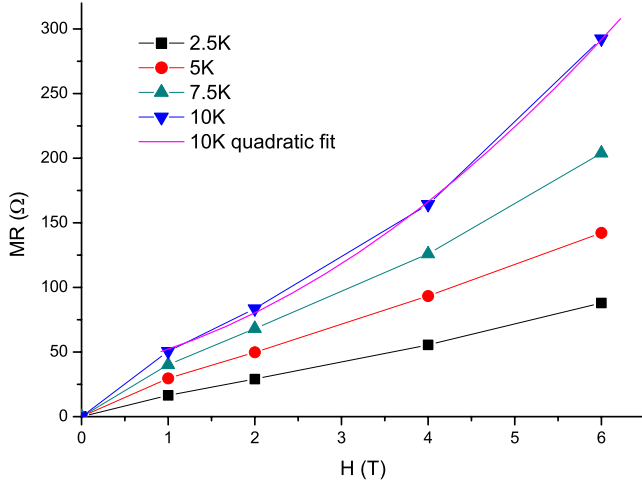


FIG. 5. (Color online) Magnetoresistance as a function of magnetic field at a few temperatures. The straight lines are just connecting the data points, while the parabolic curve is a quadratic fit to the data at 10 K for fields of 1–6 T.

a constant as assumed for low fields by the theory, but has a small decreasing contribution of about 30% with increasing magnetic field. This behavior can be explained by the effect of decreasing barrier height for vortex tunneling when the vortex-vortex interaction is increased with increasing field.

Next, we make a consistency check of our data at  $H=2$  T with Eq. (3). From the data of Fig. 2, just below  $T_c$ , we find that the pinning energy of our films is  $U_0 = V \approx 550$  K. For  $\delta\bar{V}$  of about 10% of  $V$ , one gets  $\delta\bar{V} \approx 55$  K. The measured  $T_0$  from the inset of Fig. 3 at 2 T is  $3.8^3 \approx 55$  K. Thus, for our data, Eq. (3) implies that  $\pi n_s \approx n_{pin} N_{layers}$ . For pairs,  $n_s$  equals half the doping  $p$  per copper in the  $\text{CuO}_2$  plane. In our 60 K YBCO phase,  $p \approx 0.12$ ,<sup>10</sup> which yields  $n_s \approx 0.06$  per copper. Thus,  $n_{pin} \approx \pi 0.06 / 170$  per copper in a single  $\text{CuO}_2$  plane, where  $N_{layers} \approx 170$  is the number of  $\text{CuO}_2$  planes in the 100 nm thick YBCO film. This implies that the average distance between pinning sites in a single  $\text{CuO}_2$  plane is  $l_{2D} \approx 3.9 / \sqrt{\pi 0.06 / 170} \approx 117$  Å, which is very reasonable (the 3.9 Å here is the in-plane lattice constant of YBCO).

In Fig. 5, we plot the measured magnetoresistance MR versus magnetic field for a few temperatures. One can see that at the low temperatures of 2.5 and 5 K, the MR is almost linear in field. In contrast, at higher temperatures, the dependence on the field is more complex, as seen from the data at 7.5 and 10 K. The linear MR dependence on field at a constant temperature can be attributed to a constant terminal vortex velocity in the YBCO film. This would give rise to an induced voltage across the meander line which increases linearly with field. The behavior of the MR at higher temperatures and higher fields can originate in the weak links which are distributed along the meander line. Under these conditions, the weak links become normal, and this gives rise to an MR which reflects the distribution of the strength of the weak links which can be quite complex.

Next, we point out that the main difference between the present study and the work on the vortex glass dynamics<sup>6</sup> is

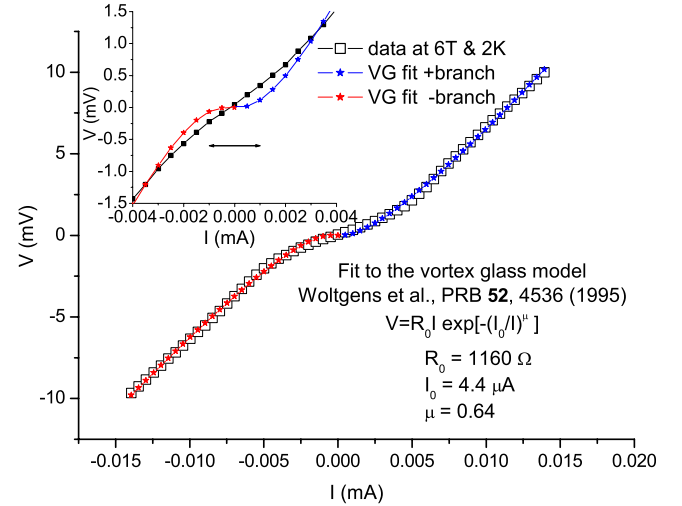


FIG. 6. (Color online) Voltage versus current curve of our meander line obtained at 2 K and field of 6 T, together with fits to the vortex glass (VG) model (Ref. 11). The inset is a zoom-in on the low bias regime.

that here we probed the low field (low vortex density) regime. The single vortex tunneling theory<sup>7</sup> predicts a magnetoresistance linear in  $H$ , as observed in Fig. 5, and ignores vortex interaction effects which are of higher order in the magnetic field. Experimentally, this is justified since at the highest field used of 6 T, the distance between vortices is of about 20 nm, while the distance between pinning sites in the whole film is only  $117 / \sqrt{170} \approx 0.9$  nm. Therefore, collective tunneling effects might well be relevant only at high fields and temperatures. Since our experiment probes the low field regime (much lower than  $H_{c2}$ ), we expect single vortex variable range hopping to dominate our results.

Finally, we make a comparison between our data and the results obtained using the vortex glass (VG) model.<sup>11</sup> Using their Eq. (7), we fit a typical  $I$ - $V$  curve of our meander line at 2 K and 6 T. The results are shown in Fig. 6 which includes the VG model fitting formula and the fitting parameters. One can see in the main panel that the VG model fits our data reasonably well at relatively high currents, while it fails badly at low currents (see the inset). Since all our resistance measurements in the present study were obtained in the low current regime of  $\pm 1$   $\mu\text{A}$  (shown by the double arrow in the inset), we conclude that the VG model is inappropriate to describe our results. In this regime, the VG model seems to yield critical-current-like behavior, while our data are clearly Ohmic-like, with the voltage linear in the current. The experimental data of the linear resistance  $R_{lin}$  versus  $1/T$  of Ref. 11 on very thin films show deviations from Arrhenius activation. These are interpreted in terms of the VG model as indicative of quantum vortex tunneling although the  $1/T$  exponents found do not yield the expected 0.7 value. Thus, the VG model is not so good to describe these experimental data either. We therefore conclude that classical activation processes and glassy dynamics (the alternative explanations to the VRH model used presently<sup>7</sup>) decisively fail to fit our data.

In conclusion, vortex variable range hopping in two di-

mensions is consistent with our experimental magnetoresistance results in a long meander line of underdoped YBCO thin films at low temperatures.

A.A. acknowledges useful discussions with Steve Kivelson and Bert Halperin. This research was supported in part

by the Israel Science Foundation (Grant No. 1564/04), the US-Israel Binational Science Foundation, the Heinrich Hertz Minerva Center for HTSC, the Karl Stoll Chair in advanced materials, and the Fund for the Promotion of Research at the Technion.

---

\*gkoren@physics.technion.ac.il; <http://physics.technion.ac.il/~gkoren>

<sup>1</sup>T. T. M. Palstra, B. Batlogg, L. F. Schneemeyer, and J. V. Waszczak, *Phys. Rev. Lett.* **61**, 1662 (1988).

<sup>2</sup>P. W. Anderson and Y. B. Kim, *Rev. Mod. Phys.* **36**, 39 (1964).

<sup>3</sup>Y. Yeshurun and A. P. Malozemoff, *Phys. Rev. Lett.* **60**, 2202 (1988).

<sup>4</sup>J. Goeke, G. F. Hanne, and J. Kessler, *Phys. Rev. Lett.* **61**, 58 (1988).

<sup>5</sup>T. Stein, G. A. Levin, C. C. Almasan, D. A. Gajewski, and M. B. Maple, *Phys. Rev. Lett.* **82**, 2955 (1999).

<sup>6</sup>M. P. A. Fisher, T. A. Tokuyasu, and A. P. Young, *Phys. Rev. Lett.* **66**, 2931 (1991).

<sup>7</sup>A. Auerbach, D. P. Arovas, and S. Ghosh, *Phys. Rev. B* **74**, 064511 (2006).

<sup>8</sup>T. T. M. Palstra, B. Batlogg, R. B. Van Dover, L. F. Schneemeyer, and J. V. Waszczak, *Phys. Rev. B* **41**, 6621 (1990).

<sup>9</sup>R. Gross, P. Chaudhari, D. Dimos, A. Gupta, and G. Koren, *Phys. Rev. Lett.* **64**, 228 (1990).

<sup>10</sup>Y. Ando and K. Segawa, *Phys. Rev. Lett.* **88**, 167005 (2002).

<sup>11</sup>P. J. M. Wöltgens, C. Dekker, R. H. Koch, B. W. Hussey, and A. Gupta, *Phys. Rev. B* **52**, 4536 (1995).